

Table S2. Antibodies and immunostaining conditions.

Antibody	Clone (Source)	Primary Antibody (Dilution/Time)	Antigen Retrieval	Detection System / IHC Platform
TBX21	4B10 (SantaCruz)	1:250 15 mins	Epitope Retrieval-ER2 (pH 9) 30 mins	Refine Detection System (Leica) / Leica Bond-III (Leica Biosystems, Buffalo Grove, IL)
CXCR3	1C6/CXCR3 (BD Pharmingen)	1:125 60 mins	CC1 (pH 8.5) 24 mins	Optiview DAB IHC Detection System without amplifier / Ventana DISCOVERY ULTRA instrument (Ventana Medical Systems, Inc, Tucson, AZ)
GATA3	L50-823 (Roche Tissue Diagnostics)	RTU 40 mins	CC1 (pH 8.5) 40 mins	Optiview DAB IHC Detection System without amplifier / Ventana DISCOVERY ULTRA instrument (Ventana Medical Systems, Inc, Tucson, AZ)
CCR4	Polyclonal (Catalog# nbp1-86584)	1:50 60 mins	CC1 (pH 8.5) 24 mins	Optiview DAB IHC Detection System without amplifier / Ventana DISCOVERY ULTRA instrument (Ventana Medical Systems, Inc, Tucson, AZ)

RTU: ready to use

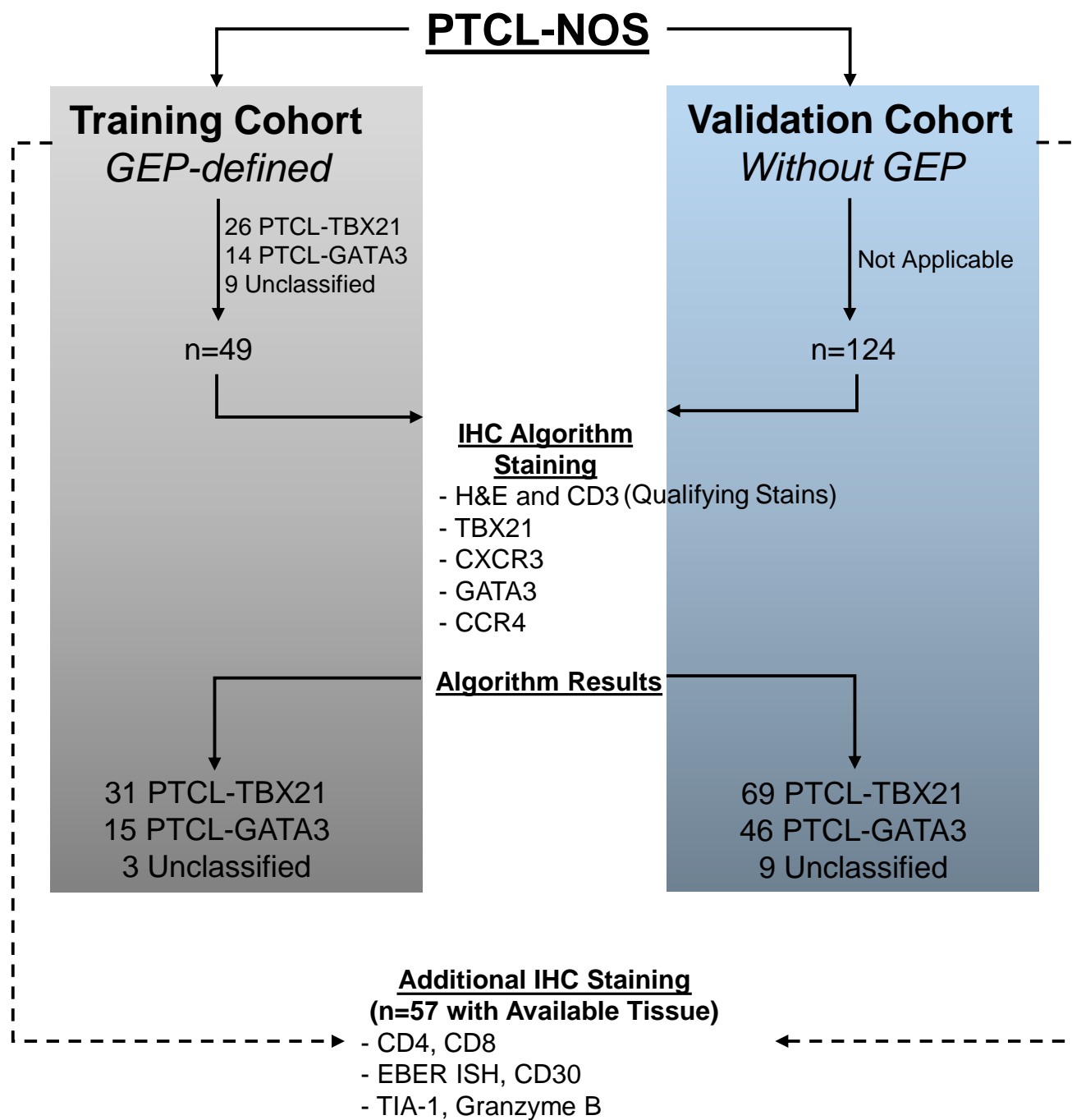
Table S3. Comparison of IHC marker positivity by GEP subgroup classification in the training cohort.

		Molecular Diagnosis by GEP							
		PTCL-GATA3 (n=14)		PTCL-TBX21 (n=26)		Unclassifiable (n=9)		Total (n=49)	
GATA3	< 50%	3 (21.4%)		15 (57.7%)		2 (22.2%)		20 (40.8%)	
	≥50%	11 (78.6%)		11 (42.3%)		7 (77.8%)		29 (59.1%)	
TBX21	< 20%	13 (92.9%)		8 (30.8%)		5 (55.6%)		26 (53.1%)	
	≥20%	1 (7.1%)		18 (69.2%)		4 (44.4%)		23 (46.9%)	
CCR4	< 50%	n= 12	2 (16.7%)	n= 20	11 (55.0%)	n= 8	3 (37.5%)	n= 40	16 (40.0%)
	≥50%		10 (83.3%)		9 (45.0%)		5 (62.5%)		24 (60.0%)
CXCR3	< 20%	13 (92.9%)		5 (19.2%)		3 (33.3%)		21 (42.9%)	
	≥20%	1 (7.4%)		21 (80.8%)		6 (66.7%)		28 (57.1%)	

GEP: Gene Expression Profiling.

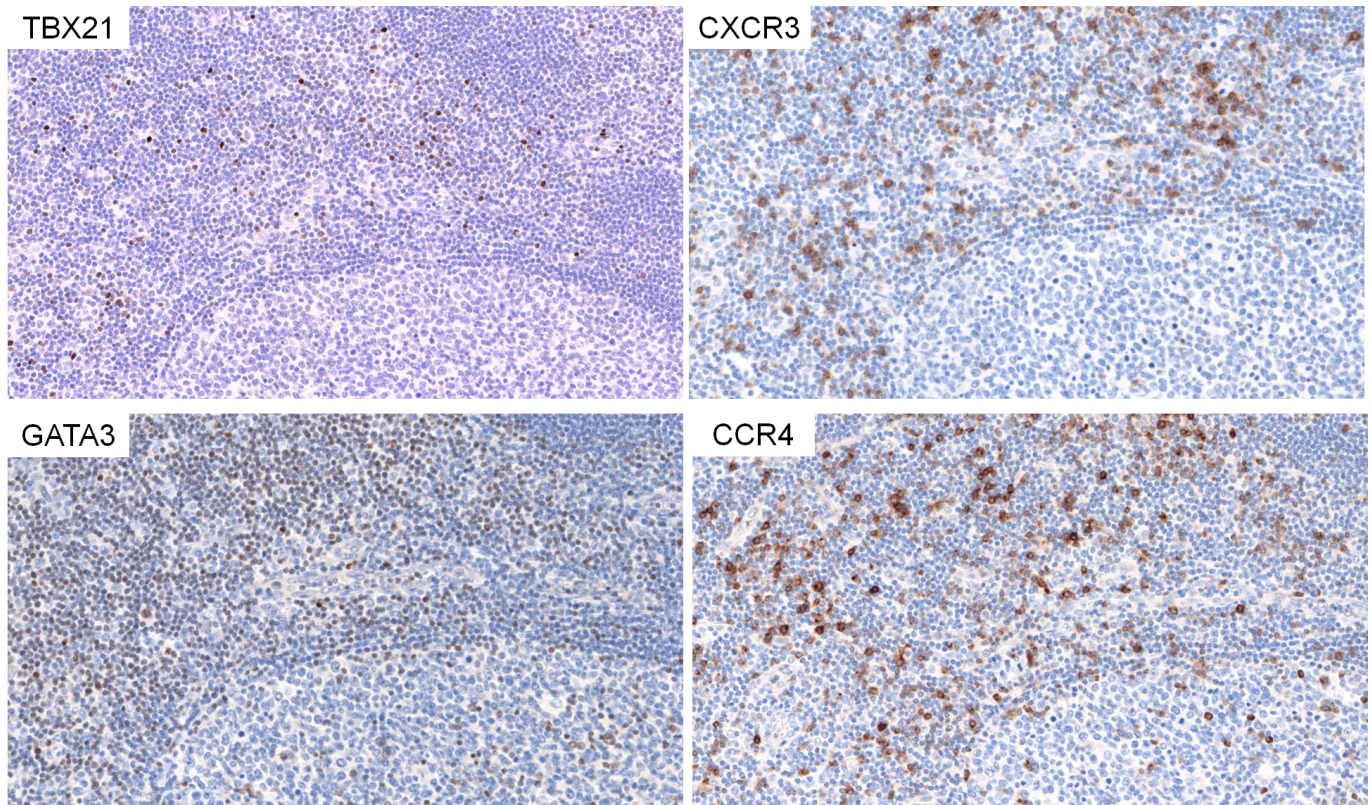
Table S4. Comparison of IHC markers and subtype characteristics by cohort.

		COHORT		p-value
		Training (n=49)	Validation (n=124)	
GATA3	< 50%	20 (40.8%)	35 (28.2%)	0.11
	≥50%	29 (59.2%)	89 (71.8%)	
TBX21	< 20%	26 (53.1%)	77 (62.0%)	0.28
	≥20%	23 (46.9%)	47 (38.0%)	
CCR4	< 50%	16 (40.0%)	51 (53.1%)	0.16
	≥50%	24 (60.0%)	45 (46.8%)	
		n=40	n= 96	
CXCR3	< 20%	21 (42.9%)	64 (51.6%)	0.30
	≥20%	28 (57.1%)	60 (48.4%)	
IHC Classification	PTCL-GATA3	15 (30.6%)	46 (37.1%)	0.65
	PTCL-TBX21	31 (63.3%)	69 (55.7%)	
	Unclassifiable	3 (6.1%)	9 (7.3%)	



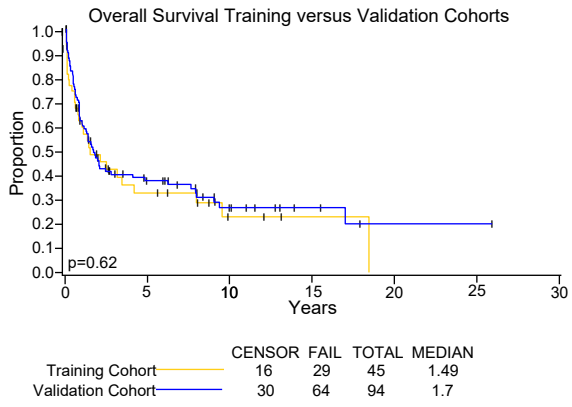
Supplemental Figure 1: Diagram of the study for inclusion of the cases in the training and validation cohorts and additional immunophenotyping.

Supplemental Figure 2

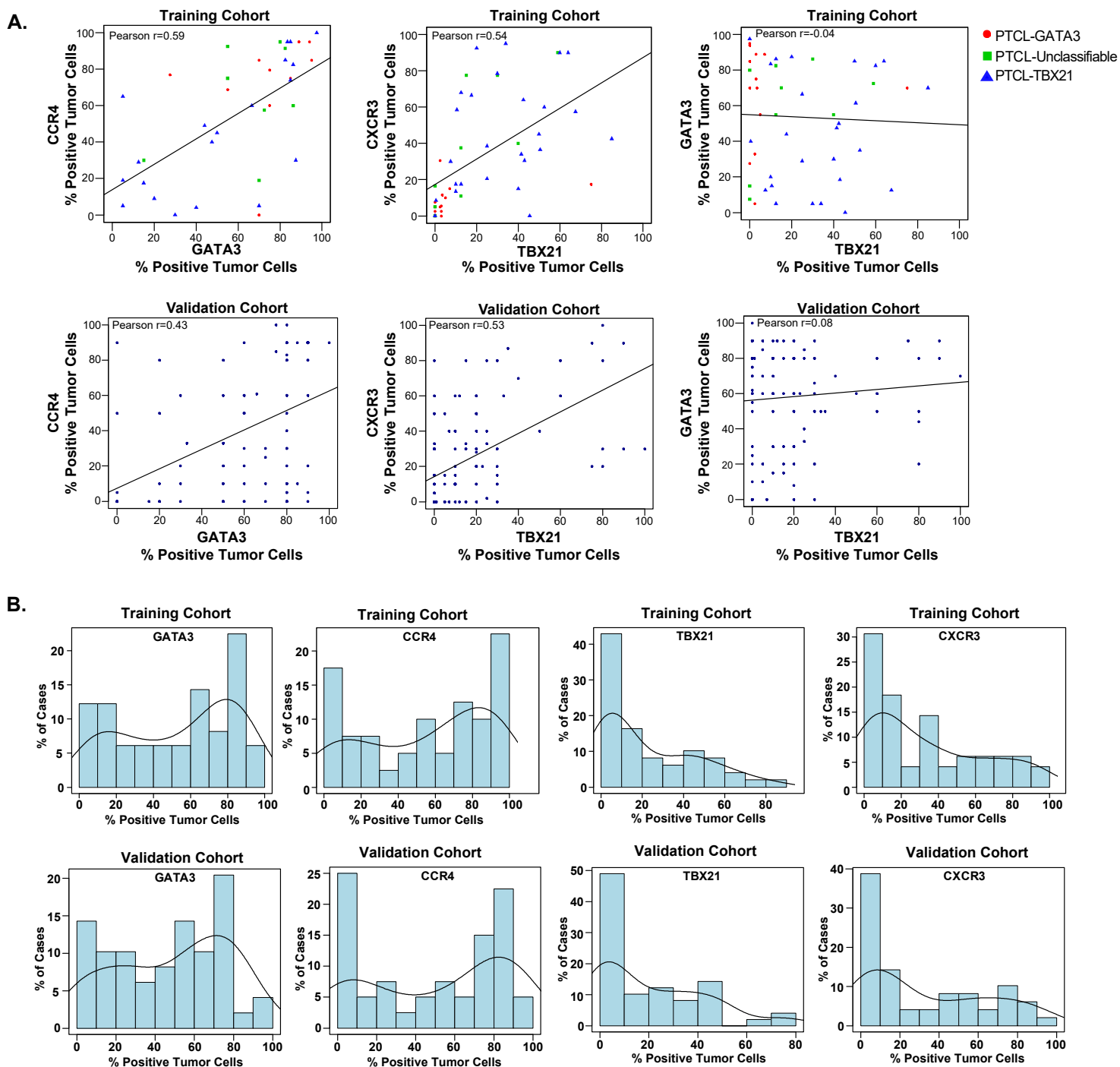


Supplemental Figure 2: Standardization of the immunostains for the IHC algorithm in tonsil tissue.
Note the nuclear staining for TBX21 and GATA3, and membranous staining for CXCR3 and CCR4.

Supplemental Figure 3



Supplemental Figure 3: Overall survival of the training and validation cohorts. Similar OS was observed between the training and the validation cohorts.

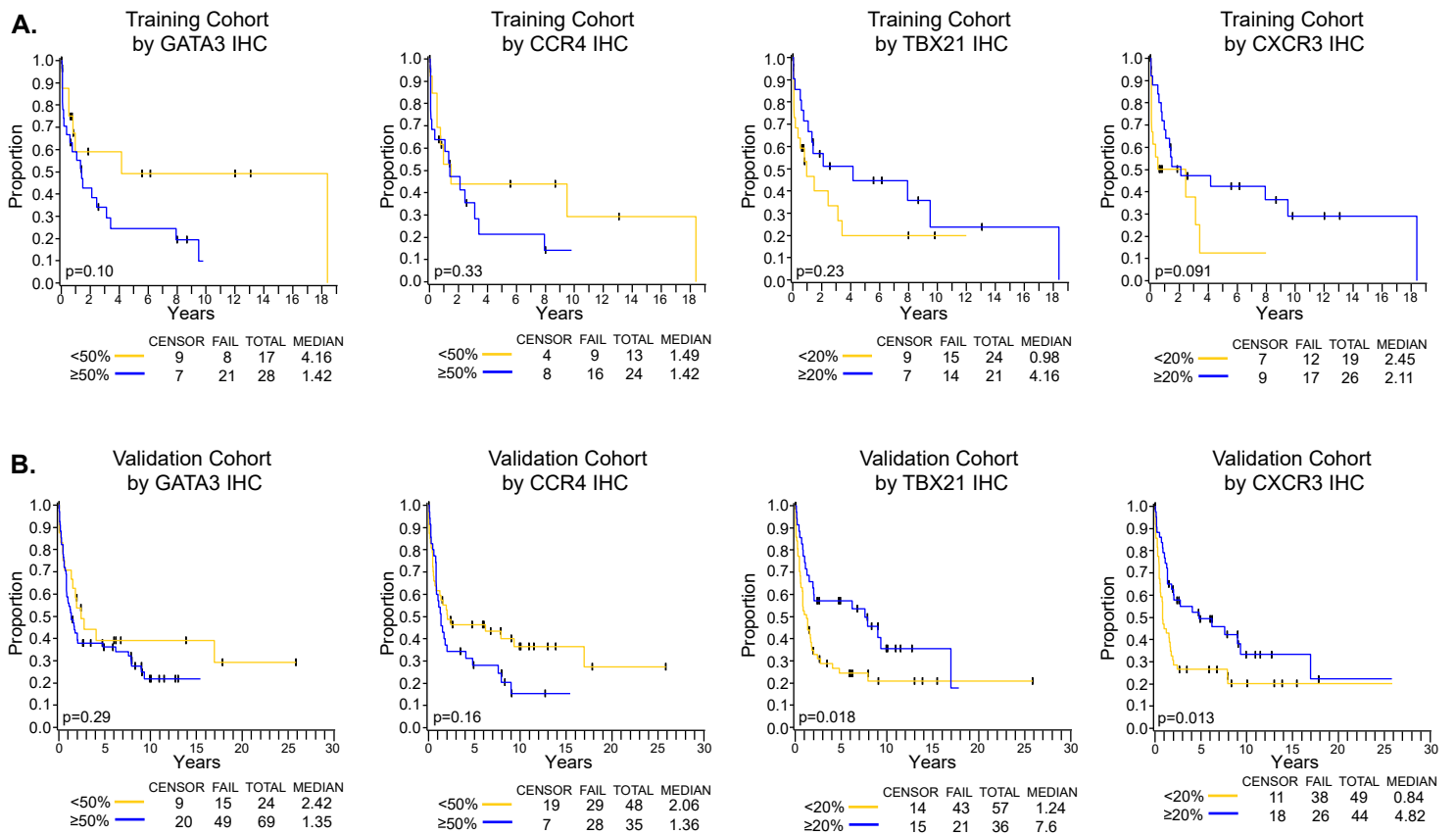


Supplemental Figure 4

4A: Correlation between expression of the transcription factors (GATA3 and TBX21) and their target proteins (CCR4 and CXCR3, respectively) in corresponding cases. Positive correlation was observed between GATA3 and CCR4, and between TBX21 and CXCR3 in the training and validation cohorts. No correlation was observed between TBX21 and GATA3.

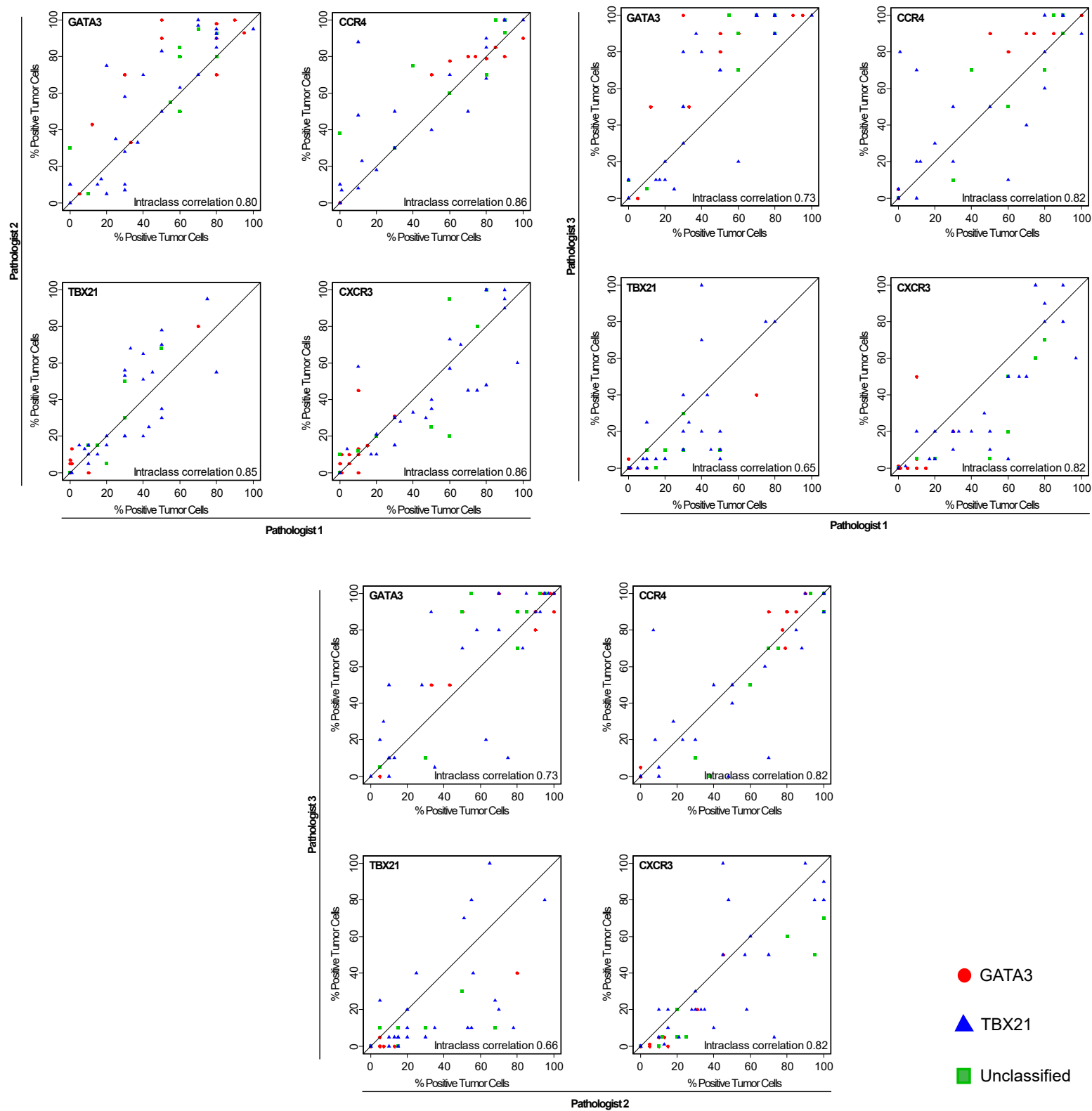
4B: Distribution of positivity of the different immunostains for the four selected antibodies. Similar trends of positivity were observed between GATA3 and CCR4. Less than 25% of the PTCL-NOS cases showed no or low expression of either GATA3 or CCR4, whereas ~50% of the cases showed no or low expression of TBX21 and CXCR3.

Supplemental Figure 5



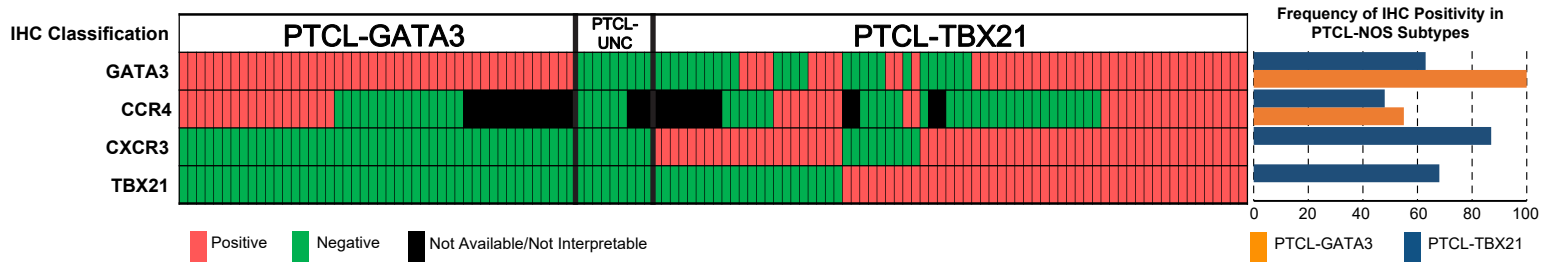
Supplemental Figure 5: Correlation of individual immunostains with overall survival. Similar trends of OS were observed for all IHC stains in the training (A.) and validation (B.) cohorts. TBX21 and CXCR3 showed a significant association with OS in the validation cohort, but not observed in the training cohort.

Supplemental Figure 6



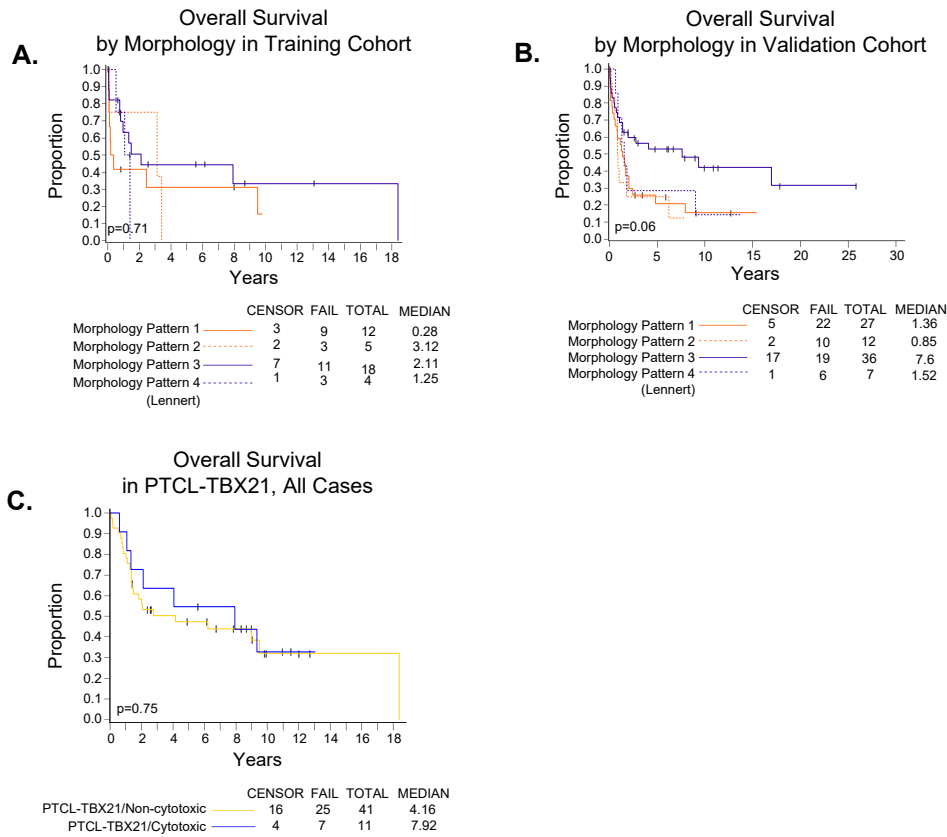
Supplemental Figure 6: Intraclass correlation of immunostains between three independent pathologists analyzed in pairs. Moderate to strong concordance was observed for the four immunostains.

Supplemental Figure 7



Supplemental Figure 7: Heatmap representation of algorithm immunostains and IHC algorithm classification in validation cohort cases. The frequency of the individual immunostain positivity in the validation cohort in the PTCL-subtypes is shown on the right.

Supplemental Figure 8



Supplemental Figure 8: Association of overall survival with morphological patterns (A-B) and with a cytotoxic phenotype (C). A non-significant trend ($p=0.06$) towards inferior OS was observed in the validation cohort for the monomorphic (1 and 2) and Lennert patterns, but was not significant in the training cohort (A-B). No difference in OS was observed in the cases with a cytotoxic immunophenotype when compared to non-cytotoxic PTCL-TBX21 (C).

Please find a list of the current Lymphoma/Leukemia Molecular Profiling Project (LLMPP) members:

Catalina Amador
Rita Braziel
Elias Campo
Wing (John) Chan
James Cook
Jan Delabie
Pedro Farinha
Andrew L. Feldman
Kai Fu
Betty Glinsmann-Gibson
Timothy Greiner
Harald Jr. Holte
Giorgio Inghirami
Javeed Iqbal
Elaine Jaffe
Pedro Jares
Sarah Ondrejka
German Ott
Stefania Pittaluga
Phil Raess
Lisa Rimsza
Andreas Rosenwald
Kerry Savage
David Scott
Graham Slack
Erlend B. Smeland
Joo Song
Lou Staudt
Dennis Weisenburger
George Wright